Sensors and Actuators B 133 (2008) 682–686

Contents lists available at ScienceDirect

Sensors and Actuators B: Chemical

journal homepage: www.elsevier.com/locate/snb

Electrochemical and geometrical characterization of iridium oxide electrodes in stainless steel substrate

Carmen C. Mayorga Martinez[a,b,*], Rossana E. Madrid[a,b], Carmelo J. Felice[a,b]

[a] Departamento de Bioingeniería (DBI), Facultad de Ciencias Exactas y Tecnología (FACET), Universidad Nacional de Tucumán (UNT), CC 327-Correo Central (4000) Tucumán, Argentina
[b] Instituto Superior de Investigaciones Biológicas (INSIBIO), Consejo Nacional de Investigaciones Científicas y Técnicas (CONICET), CC 327-Correo Central (4000) Tucumán, Argentina

ARTICLE INFO

Article history:
Received 17 December 2007
Received in revised form 18 March 2008
Accepted 28 March 2008
Available online 8 April 2008

Keywords:
EIROF layers
Electrode–electrolyte impedance
Randles model
Iridium oxide

ABSTRACT

A geometrical and electrochemical characterization of stainless steel electrodes electrodeposited with iridium oxide (IrO_2) is presented. There is a dramatic increase in the double layer capacitance (C) and an important decrease in the charge transfer resistance (R_{ct}) after electrodeposition, causing also a significant two orders of magnitude reduction of the electrode–electrolyte interface impedance (EEIZ). These phenomena may be explained by the fine-grained iridium oxide, which has a high grain boundary density and which increases the actual electrodic area. An RC model is presented, which would explain the electrical behaviour of the system.

1. Introduction

Metallic electrodes are used as transducers for ions in electronic currents. Since electrode–electrolyte interface impedance (EEIZ) distorts the measurements, it becomes very important to diminish it. This EEIZ influence is more significant as the area of the electrodes gets smaller. This is the case, for example, of the electrodes used in biosensors, which are generally very small. The EEIZ reduction could be achieved by increasing the area with physical methods or by chemical modification of the surface, like electrodeposition of oxide films. These surface modifications might not alter the redox reactions and chemical phenomena occurring in this electrode electrolyte interface (EEI). It is reported that the iridium oxide decreases the EEIZ [1]. This oxide also presents a good conductivity (metallic type) and has a rutile-type structure.

Iridium oxide has been used in biosensors as electrodes where enzymes can be immobilized [2]. Due to its low EEIZ, miniaturization is possible. Electrodeposited iridium oxide films (EIROF) electrodes used as pH electrodes were also reported, because the half cell potential of the oxide–electrolyte interface is sensitive to pH changes in the solution [3–8]. It is also used to coat stimulation electrodes due to its low EEIZ [1].

The methods for the formation of iridium oxide include electrodeposition on metallic surfaces to form electrodeposited iridium oxide films, thermal decomposition of iridium salts to form thermal iridium oxide films (TIROFs), reactive sputtering to form sputtered iridium oxide films (SIROFs) and activated iridium oxide films (AIROFs) formed from Ir wire [1,3,4,9]. In all the cases, the resulting solid predominantly contains IrO_2, which has an oxidation state of +4, and shows great stability in a wide range of pH even at high temperatures (up to 250 °C) and high pressure [4–11]. The electrodeposition processes mainly require solutions composed of complex mixtures of substances [12]. The most important substance is the deposition ionic source, which in the present case is the $IrCl_4$.

The potentiodynamic technique, described by Yamanaka (1989), is applied on noble metals and stainless steel substrates. Meyer et al. tested different metallic substrates to fabricate EIROF electrodes for neural stimulation and recording electrodes, where stainless steel substrate had lower performance [1]. The description of different techniques in order to obtain iridium oxide films has been reported. Nevertheless, the causes of EEIZ reduction has not been found in literature. It would be helpful to improve procedures to obtain lower impedance, more stable and easy to fabricate electrodes.

Although electrodeposition of noble metals, such as iridium, platinum, gold or titanium, has been reported, this tends not to have been on stainless steel. This material has a high EEIZ, but it is possible to reduce it by electrodepositing IrO_2 on the surface. To

* Corresponding author at: Departamento de Bioingeniería (DBI), Facultad de Ciencias Exactas y Tecnología (FACET), Universidad Nacional de Tucumán (UNT), CC 327-Correo Central (4000) Tucumán, Argentina. Tel.: +54 381 4364120; fax: +54 381 4364120.
E-mail address: carmen.mayorga@gmail.com (C.C. Mayorga Martinez).

0925-4005/$ – see front matter © 2008 Elsevier B.V. All rights reserved.
doi:10.1016/j.snb.2008.03.037

obtain very low EEIZ on stainless steel electrodes and to understand the origin of this reduction upon IrO_2 deposition is the main interest of this paper. Meyer's protocol is modified, in order to optimise the EIROF over stainless steel substrate.

The evaluation is made using electrical and geometrical characterization by electrochemical impedance spectroscopy (EIS) and scanning tunneling microscopy (STM). A dramatic increase in the double layer capacity (C) and an important decrease in the charge transfer resistance (R_{ct}) (parameters not previously evaluated in the bibliography) are obtained, causing a reduction of two orders of magnitude in the EEIZ, similar to that found in the literature [1]. These phenomena are explained by the EIROF microscopic characteristics.

2. Materials and methods

The electrodeposition solution contains hydrated iridium tetrachloride $IrCl_4$ 99.9% (Aldrich), dihydrated oxalic acid 99.5% (Fluka) and anhydrous potassium carbonate K_2CO_3 99.0% (Fluka). Sodium chloride (Ciccarelli) is used for the impedance measurements. All the solutions should be prepared with distilled water (5 μS).

A glass tripolar cell is employed for the electrodeposition (Fig. 1). It has a stainless steel hemispherical counter-electrode, 85 mm in diameter, and an Ag/AgCl reference electrode. The working electrodes are stainless steel AISI 316L cylinders electrodeposited with IrO_2, mounted in acrylic, leaving a circular exposed area of 1.27 cm^2.

The measurements are carried out with the Solartron® system 12508 W, which includes a Frequency Response Analyzer 1250 and an electrochemical interface 1287. The data visualization and processing are carried out with Solartron's commercial system Software CorrView® and Zview®.

In order to analyse the reduction of the EEIZ after the formation of EIROF, the impedance module relationship before (Z_b) and after (Z_a) the electrodeposition, measured at 1 Hz, is evaluated and expressed as Z_b/Z_a. The use of this frequency is because this parameter is important at low frequencies. Many biological signals are found in this range.

R_{ct} and C are deduced from the Randles model by using the following equation:

$$Z = R_b + \frac{Xc^2 R_{ct}}{R_{ct}^2 + Xc^2} - \frac{iXc\,R_{ct}^2}{R_{ct}^2 + Xc^2}$$

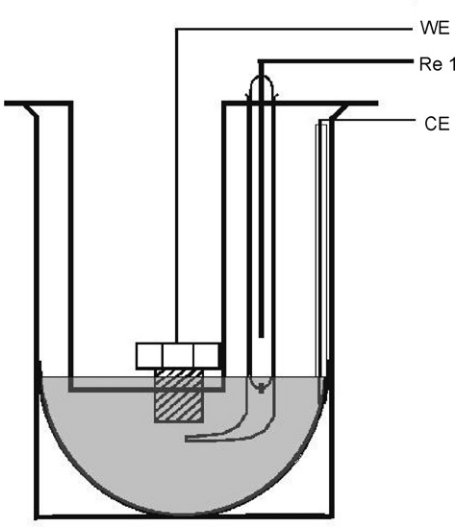

Fig. 1. Electrodeposition cell (WE, working electrode; Re1, reference electrode; CE, counter electrode).

Table 1
Polishing protocol

Steps	Abrasive	Grain size (μm) FEPA[a]
1	Sandpaper 120 BUEHLER®	127
2	Sandpaper 240 BUEHLER®	58.5
3	Sandpaper 400 BUEHLER®	35
4	Sandpaper 600 BUEHLER®	15.3
5	Diamond paste Prazis® and polishing cloth No. 40-7068	6
6	Diamond paste Prazis® and polishing cloth No. 40-7068	3
7	Alumina powder Prazis® and polishing cloth No. 40-7218	1

[a]The grain size corresponds to the European FEPA Standard 43-GB-1984 (R1993) [14].

In this case, the model does not includes the Warburg impedance, because diffusion is negligible due to the support electrolyte used [13]. The calculation is made by using MathCad 8.0. Other evaluated relationships are the decrease of R_{ct} before and after the electrodeposition (R_{ctB}/R_{ctA}) and the increase of C after and before the electrodeposition (C_a/C_b).

A thermostatized bath is used to maintain the temperature at 30 ± 0.2 °C during the electrodeposition process. The electrodes are polished with a home made metallographic polisher, which has a head speed of 280 rpm, an integrated lubricant dispenser system and exchangeable polishing discs.

The STM measurements are performed with a Molecular Imaging microscope (Phoenix, Arizona), using tungsten tips electrochemically etched from a 0.25 mm diameter. GWYDDION v. 2.5 software is used for the digital image processing.

The statistical analysis is made with GraphPad Pism v. 3.00 Software. One-way Anova statistical test, with a confidence interval of 0.95, is employed to evaluate the surface roughness effect on the obtained EIROF.

2.1. Electrode fabrication and polishing

The electrodes are polished following Table 1, by using sandpaper of different roughness, diamond paste and alumina dust to obtain surfaces of different roughness. Steps 1–4 are carried out with the metallographic polisher, while the subsequent ones are hand made using polishing cloths and their corresponding abrasives. Finally the electrodes are cleaned with distilled water and isopropyl alcohol.

Five different analyses are made, using groups of electrodes of 12.7 mm in diameter with the characteristics described in Table 2.

2.2. Electrodeposition

The electrodeposition solution is prepared by dissolving 4 mmol/L $IrCl_4$ in 40 mmol/L oxalic acid, followed by the slow addition of 340 mmol/L K_2CO_3 to a final pH of 10.3 [1]. Then, it is magnetically stirred until all the components are dissolved. The solution is allowed to sit quiescently at room temperature in the dark for 8 days until it turns blue. At this moment, it is ready to be stored at 4 °C up to 2 or 3 weeks prior to use [6]. It is possible to employ a modified protocol to prepare the solution, which reduces the time preparation [5].

A potentiodynamic known technique is employed for the electrodeposition [1], but with some modifications. They were made in order to achieve better EIROF characteristics over stainless steel. It consists of the combination of potential cycling with a triangular wave (50 cycles between 0.0 and 0.55 V versus the Ag/AgCl reference electrode at a 50 mV/s sweep rate) followed immediately

Table 2
Description of the groups employed in the different analysis of this paper

Group No.	Analysis	No. of electrodes	No. of step according to Table 1
1	Analysis of C, R_{ct} and Z	4	6
2	Analysis to different roughness	6 6 6	1 4 6
3	STM images	2	6

by rectangular potential pulsing (same potential limits for up to 3000 pulses of 0.5 s each). The electrodeposition takes place in a water bath at 30 °C. Finishing the protocol, the electrodes are kept submerged for 45 min to be finally stored in the dark at room temperature. The original protocol makes the electrodeposition at room temperature, does not let the electrodes to rest inside the solution after electrodeposition and uses 1600 pulses.

Impedance is measured before and after electrodeposition in a tripolar cell by applying 10 mV (RMS) at frequencies from 0.1 to 1000 Hz. The open circuit potential is previously registered until the variations are below 0.05 V for 30 s, to verify that the EEI is stable. Measurements are made in a 0.9% NaCl solution (12 mS) at room temperature.

2.3. Surface morphology and microstructure

STM images are obtained for two electrodes, one with EIROF and the other one over the stainless steel substrate (group 3, Table 2), previously cleaned with methanol. Gwyddion® free Software is used for image processing.

3. Results

Fig. 2 shows the comparison between the relationships of impedances before (Z_b) and after (Z_a) electrodeposition measured at 1 Hz, capacitances before (C_b) and after (C_a) electrodeposition and charge transfer Resistance before (R_{ctB}) and after (R_{ctA}) electrodeposition, using the electrodes of group 1, Table 2.

Fig. 3 shows the impedance module for electrodes of different roughness measured at 1 Hz before and after the electrodeposition (group 2, Table 2). The impedance values measured before the electrodeposition were between 2.5 and 4 kΩ, but after that, all these values are around 70 Ω. When applying the one-way ANOVA statistic analysis, the mean values were different, $p = 0.0024$ for Z_b, whereas these means remain stable ($p = 0.66$) for Z_a.

Fig. 4 shows the impedance module and phase with respect to the frequency before and after electrodeposition of an electrode

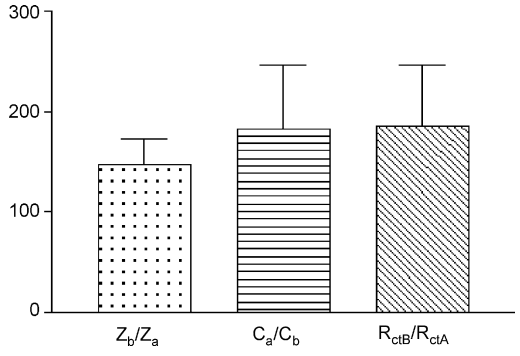

Fig. 2. Comparison between the relationships of impedances before (Z_b) and after (Z_a) electrodeposition measured at 1 Hz, capacitances before (C_b) and after (C_a) electrodeposition and charge transfer resistance before (R_{ctB}) and after (R_{ctA}) electrodeposition.

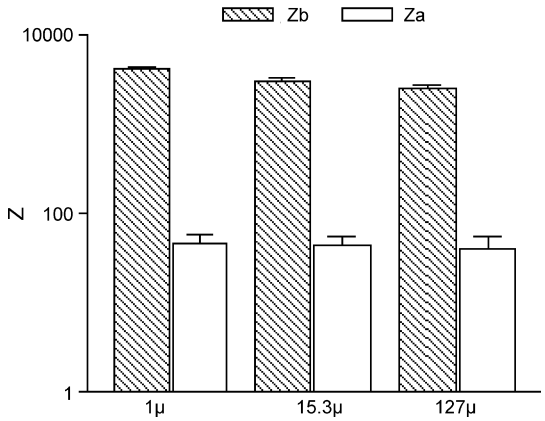

Fig. 3. Comparison of impedances before (Z_b) and after (Z_a) electrodeposition for three electrode groups polished with three different sandpapers.

polished with 1 μm alumine powder. It is observed that, at 1 Hz, the impedance module of the EIROF electrode is 72 times lower with respect to the impedance measured on the stainless steel electrode capacitive with a huge phase angle.

Fig. 5A shows the 3D image of a stainless steel electrode obtained by STM. Fig. 5B shows a lateral z plane for the same electrode. Fig. 5C and D shows the same images of Fig. 5A and B but for an EIROF electrode. It is observed that EIROF has 12% greater surface area than the stainless steel electrode. The surface area was calculated by using the triangulation scheme provided by the Gwyddion® software (Group 4, Table 2).

Fig. 6 shows the Argand diagram (plot of points $z = x + iy$ in the complex plane) for an electrode polished at 1 μm before and

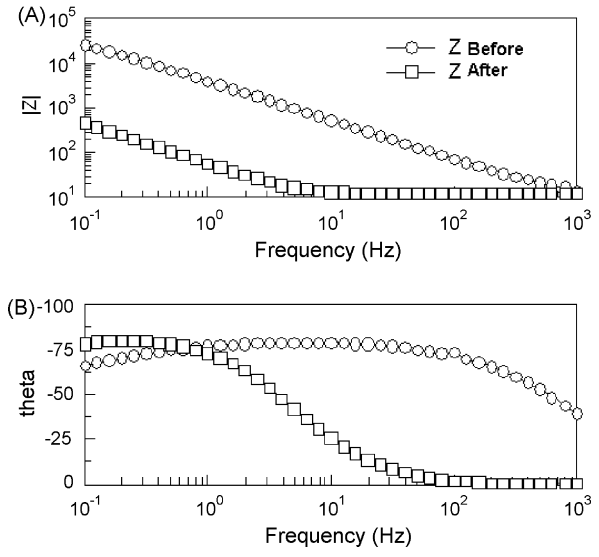

Fig. 4. (A) Total impedance module vs. frequency; (B) Phase angle vs. frequency.

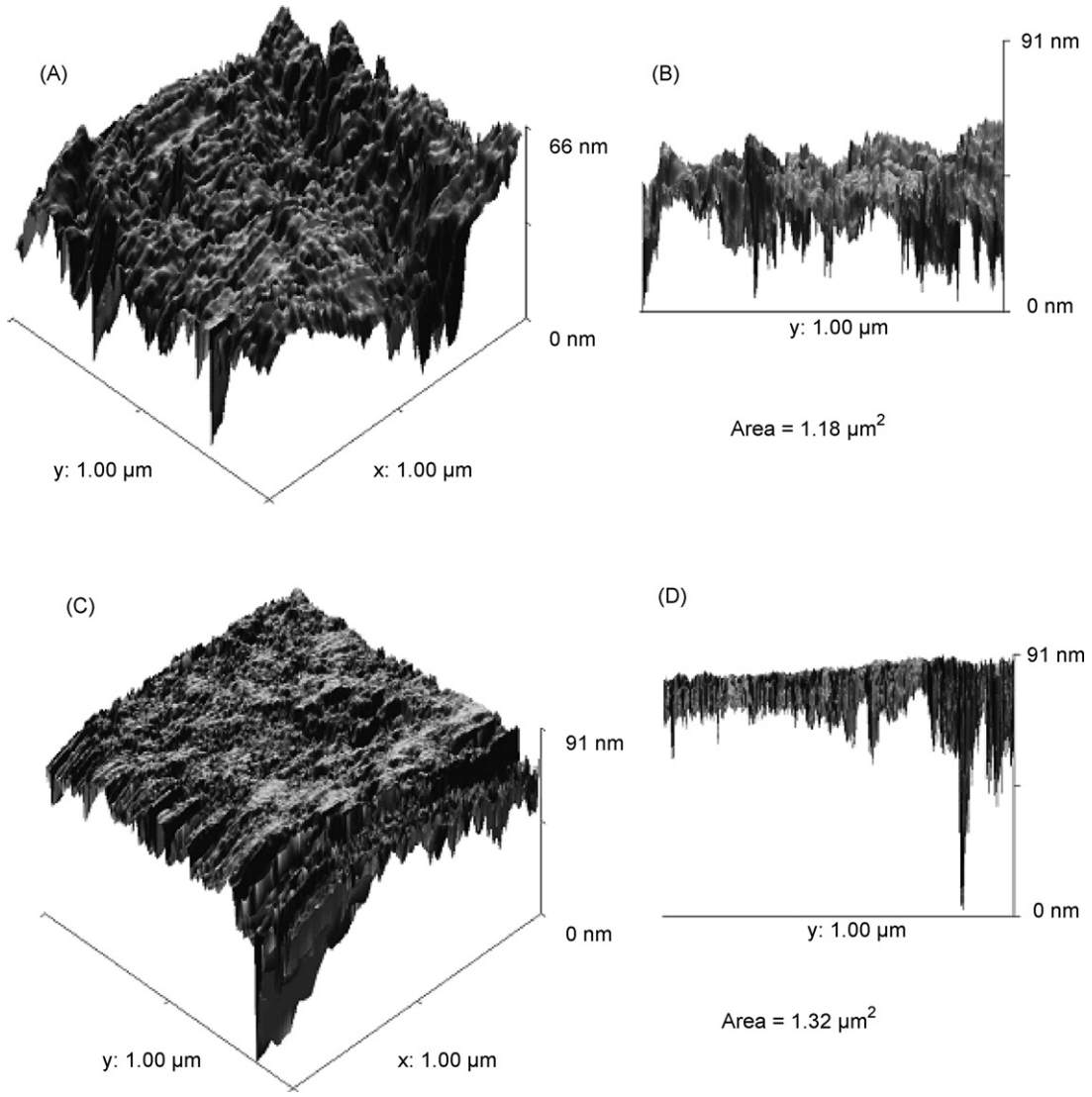

Fig. 5. (A) 3D STM image (1000 nm × 1000 nm, Bias = 0.4 V and tunnel current = 0.1 nA) of the AISI 316L stainless steel electrode surface. (B) Lateral view of the same electrode showed in (A). (C) 3D STM image (1000 nm × 1000 nm, Bias = 0.45 V and tunnel current = 0.6 nA) of the EIROF electrode. (D) Lateral view of the same electrode showed in (C).

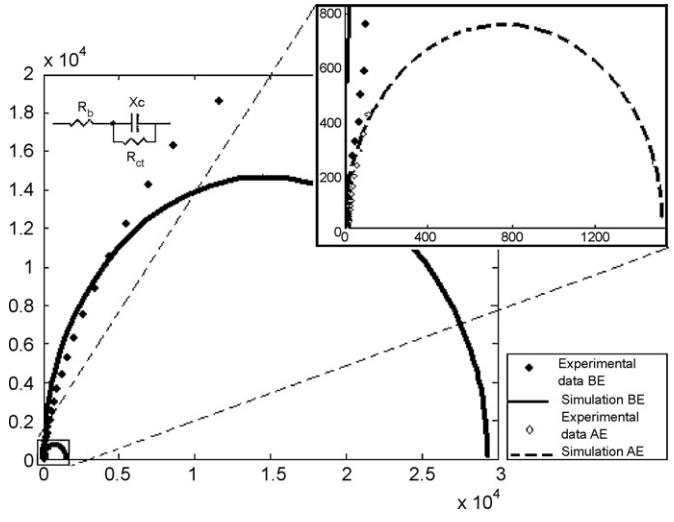

Fig. 6. Argand diagram for an electrode polished at 1 μm before and after electrodeposition (BE and AE, respectively) (R_b, bulk resistance; C, double layer capacity; R_{ct}, charge transfer resistance).

after electrodeposition. The diagram is obtained by simulation in Matlab® from the series equivalent of the Randles model [14] shown in the same figure. The bulk resistance R_b, R_{ct} and C are obtained by fitting the experimental data with software Zview®.

4. Discussion

When comparing the EEIZ before (Z_b) and after (Z_a) electrodeposition (Fig. 3), it can be deduced with statistical validity that EIROF allows to obtain similar EEIZ, thus providing reproducible surfaces. This is an important fact in applications of electrochemistry and bioengineering, because surfaces equally polished and prepared not always give the same EEIZ. The direct application is in electrodes and sensors construction. On the other hand, the electrodeposition of iridium oxide in stainless steel substrate offers a significant EEIZ reduction of two orders of magnitude, which can be observed in the Bode diagram of Fig. 4. This feature is highly appreciated in bioengineering.

In STM images a fine-grained oxide is observed after electrodeposition (Fig. 5C and D). In general terms, small grain size leads to a high grain boundary density [15]. On the other hand, in a range of

grain size between 10 and 40 nm, electronic conductivity increases by several orders of magnitude, while ionic conductivity decreases. These characteristics are attributed to space charge layers along the grain boundaries in the polycrystalline material [15]. Iridium oxide presents a grain size between 20 and 30 nm [2] and, therefore, a high grain boundary density, leading to a high electronic conductivity but low ionic conductivity [16]. Another important fact is that 0.1 nA is used to obtain STM images of stainless steel substrate, and 0.6 nA is used to obtain EIROF images, thus demonstrating the high conductivity of this material. It is possible to assume then, that the reduction on R_{ct} is due to the presence of the great electronic conductivity of this porous oxide (Fig. 2). Comparing the surface areas in the STM images of Fig. 5, an increment of this parameter is observed after electrodeposition. This increment would explain the higher value of Cdl obtained (Fig. 2).

The Argand diagram clearly shows the important reduction on R_{ct} and the increment in C. To simulate the electric behavior of this oxide, the Randles model composed by the parallel of a small R_{ct} and a big capacitor is proposed (Fig. 6). This model fits experimental data reasonable well and is employed for the comparison of these parameters before and after electrodeposition.

5. Conclusions

A stainless steel electrode with a very low EEIZ is obtained through the electrodeposition of IrO_2. The impedance module measured at 1 Hz is reduced in two orders of magnitude. The important decrease in EEIZ should be caused by the presence of the fine-grained EIROF, which have a high electronic conductivity (very low R_{ct}) and an increased surface area (big C). The formed EIROFs are easily fabricated, repeatable and stable in time. The low EEIZ obtained and the desirable characteristics achieved in a stainless steel substrate, make it a promising material to be used as the transducer for the immobilization of enzymes in biosensors. The use of a low cost substrate makes this technology more accessible.

Acknowledgments

The authors especially thank Dr. Martín Patrito from the Universidad de Córdoba, Argentina for the support with STM images and for his suggestions, Mr. Santiago Caminos for his translation assistance and Dr. Max Valentinuzzi for English correction in the final preparation of the manuscript. Supported by the Agencia Nacional de Promoción Científica y Tecnológica, the Consejo Nacional de Investigaciones Científicas y Técnicas (CONICET), Institucional funds of INSIBIO (Instituto Superior de Investigaciones Biológicas) and the Consejo de Investigaciones de la Universidad Nacional de Tucumán (CIUNT).

References

[1] R. Meyer, S. Cogan, T. Nguyen, R. Rauh, Electrodeposited iridium oxide for neural stimulation and recording electrodes, IEEE Trans. Neural. Sys. Rehabil. Eng. 9 (March (1)) (2001) 2–10.
[2] E.A. Irhayem, H. Elzanowska, A.S. Jhas, B. Skrzynecka, V. Birss, Glucose detection based on electrochemically formed Ir oxide films, J. Electroanal. Chem. 538/539 (August) (2002) 153–164.
[3] M. Petit, V. Plichon, Anodic electrodeposition of iridium oxide films, J. Electroanal. Chem. 444 (March) (1998) 247–252.
[4] S. Yao, M. Wang, M. Madou, A pH electrode based on melt-oxidazed iridium oxide, J. Electrochem. Soc. 148 (4) (2001) H29–H36.
[5] S. Marzouk, Improved electrodeposited iridium oxide pH Sensor Fabricated on Etched Titanium Substrates, Anal. Chem. 75 (March (6)) (2003) 1258–1266.
[6] I. Ges, B. Ivanov, D. Schaffer, E. Lima, A. Werdich, F. Baudenbacher, Thin-film IrO_x. pH microelectrode for microfluidic-based Microsystems, Biosens. Bioelectron. 21 (2005) 248–256.
[7] S. Marzouk, S. Ufer, R. Buck, Electrodeposited iridium oxide pH electrode for measurement of extracellular myocardial acidosis during acute ischemia, Anal. Chem. 70 (December (23)) (1998) 5054–5061.
[8] A. Bezbaruah, T. Zhang, Fabrication of anodically electrodeposited iridium oxide film pH microelectrodes for microenvironmental studies, Anal. Chem. 74 (November) (2002) 5726–5733.
[9] K. Alexandru, H. Ying-Sheng, T. Dah-Shyang, T. Kwong-Kau, Growth and characterization of well aligned densely packed IrO_2 nanocrystals on sapphire via reactive sputtering, J. Phys.: Condens. Matter 18 (2006 Feb.) 1121–1136.
[10] J. Baur, T. Spaine, Electrochemical deposition of iridium (IV) oxide from alkaline solutions of iridium (III) oxide, J. Electroanal. Chem. 443 (1998) 208–216.
[11] S. Gottesfeld, J. Mcintyre, G. Beni, J. Shay, Electrochromism in anodic iridium oxide films, Appl. Phys. Lett. 33 (July (2)) (1978) 208–210.
[12] T. Bruno, Laboratory Scale Electrodeposition, J. Chem. Educ. 63 (October (10)) (1986) 833–886.
[13] C. Gabrielli, Identification of Electrochemical Process by Frequency Response Analysis (Solution Group), ASTM Standard G106, 1980.
[14] BUEHLER Ltd., Buyer's Guide 2006/2007, http://www.buehler.com/productinfo/06_07_Euro_Consumables.pdf.
[15] A. Tschöpe, S. Kilassonia, R. Birringer, The grain boundary effect in heavily doped cerium oxide, Solid State Ionics 173 (September) (2004) 57–61.
[16] S.F. Cogan, T.D. Plane, J. Ehrlich, Sputtered iridium oxide films (SIROFs) for low-impedance neural stimulation and recording electrodes, in: Proceedings of the 26th Annual International Conference on IEEE EMBS, San Francisco, CA, USA, September 1–5, 2004.

Biographies

Carmen C. Mayorga Martinez was born in Cusco, Peru. She received the Chemical Pharmaceutical degree at the University of San Antonio Abad of Cusco-Peru in 1999. She studied a first year of the Biomedical Engineering Master at the Pontifical Catholic University of Perú in 2004. Currently she is PhD student at the University of Tucuman, INSIBIO, CONICET under the tutelage of Dr Rossana Madrid. Her main research fields include the development of Biosensor for biomedical applications as well as the study of non-linear impedance measurements as a new method of transduction.

Rossana Madrid was born in 1964. She received the Electronic Engineer degree at the University of Tucumán and her PhD in 1998 under the tutelage of Dr Valentinuzzi, for the design and development of an equipment to measure impedance and turbidity in biological suspensions. As a postdoctoral fellow, she spent a short time at the Institut für Technishe Chemie at the University of Hannover in Germany, in the group of biosensors led by Dr Thomas Scheper. She also leads degree thesis for students of electronic engineer. She is a teacher of Biomedical Transducers of the Bioengineering Master degree. Her main research fields include the development of equipments for food industry and bioprocesses as well as the study of non-linear impedance measurements in biological suspensions.

Carmelo Felice was born in Tucumán, Argentina. He received the Electronic Engineering degree form the National University of Tucumán and the PhD degree in Bioengineering from the Department of Bioengineering, National University of Tucumán in 1995. He worked in impedance microbiology. At present, his main interests are linear and non-linear dielectric spectroscopy, tissue engineering and biosensors.